J|A|C|S
COMMUNICATIONS

Published on Web 06/27/2008

Carbon Avoids Hypercoordination in CB_6^-, CB_6^{2-}, and $C_2B_5^-$ Planar Carbon−Boron Clusters

Boris B. Averkiev,[†] Dmitry Yu. Zubarev,[†] Lei-Ming Wang,[‡] Wei Huang,[‡] Lai-Sheng Wang,*[,‡] and Alexander I. Boldyrev*[,†]

Department of Chemistry and Biochemistry, Utah State University, 0300 Old Main Hill, Logan, Utah 84322, Department of Physics, Washington State University, 2710 University Drive, Richland, Washington 99354, and Chemical and Materials Sciences Division, Pacific Northwest National Laboratory, MS K8-88, P.O. Box 999, Richland, Washington 99352

Received February 19, 2008; E-mail: ls.wang@pnl.gov; a.i.boldyrev@usu.edu

In the past two decades, computational chemistry has made dramatic advances, enabling the prediction of novel molecules that often contradict chemical intuition. Many theoretical chemists have participated in this endeavor, proposing myriads of unusual molecules. However, very often the predicted species are not the global minima, and it is difficult if not impossible to observe them experimentally. Molecules with hypercoordinated carbons in planar boron−carbon clusters are vivid examples of such predictions. Here we aim to show via a joint experimental and theoretical investigation that such species are too high in energy to be experimentally observed.

Since Hoffmann and co-workers[1] proposed the idea of tetracoordinate planar carbon (tpC) molecules, there have been numerous computational predictions of such unusual species.[2−5] Ab initio predictions of thought-to-be-outlandish pentaatomic tpC molecules[6] were experimentally confirmed in 1999 and 2000.[7] These experimental advances have stimulated further searches for even higher coordination in planar carbon species.[8−10] In particular, a series of C/B binary clusters with hypercoordinate planar carbons[8a] has been proposed and has attracted significant attention.[11,12] The planar CB_6^{2-} cluster, which has a hexacoordinate carbon, has been touted as a "divining molecule" and highlighted on the cover of *Chemical & Engineering News*.[11] In this article, we show that in systems containing boron atoms as ligands, such as CB_6^{2-}, the central position with high coordination number should be favored for atoms with low electronegativities and strong tendencies to participate in delocalized bonding. The key point here is the presence of two-center, two-electron bonds between peripheral atoms. The higher electronegativity of C compared to B clearly disfavors the hexacoordinate C isomers of CB_6^- and $C_2B_5^-$. It should be pointed out that an extensive survey of the isoelectronic C_3B_4 has also revealed that the hexacoordinate isomer is higher in energy.[8a]

Heptacoordinate planar carbon in the D_{7h} CB_7^- cluster was initially predicted computationally by Schleyer and co-workers.[8b] Recently, we serendipitously observed a highly stable CB_7^- cluster during laser vaporization experiments. Using photoelectron spectroscopy (PES) and ab initio calculations, we found that the global-minimum planar structure of CB_7^- has C_{2v} symmetry with the C atom occupying a peripheral position.[13] The planar D_{7h} CB_7^- structure may be kinetically stable but has a much higher energy than the C_{2v} structure. In principle, kinetically stable but thermodynamically unfavorable isomers can be observed under some special conditions, but they were not populated under the experimental conditions of the previous study. Here we present both experimental and ab initio results demonstrating that the most stable isomers of CB_6^{2-}, its isoelectronic analogue $C_2B_5^-$, and CB_6^- are not the previously proposed planar structures containing a hexacoordinate carbon. Instead, the latter are found to be extremely high energy isomers and cannot be made through atom self-assembly in the gas phase.

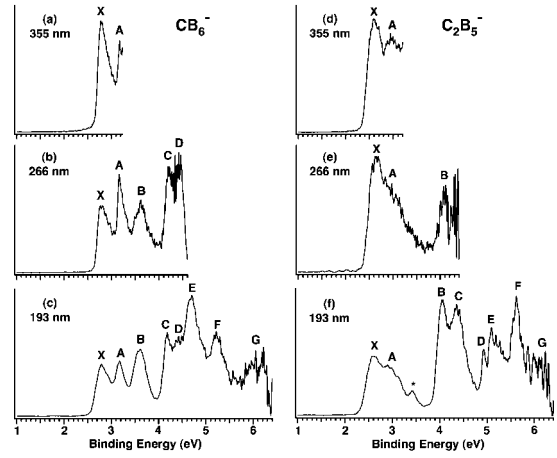

Figure 1. Photoelectron spectra of (left) CB_6^- and (right) $C_2B_5^-$ at 355 nm (3.496 eV), 266 nm (4.661 eV), and 193 nm (6.424 eV).

The experiment was performed using a laser-vaporization cluster source and a magnetic-bottle PES analyzer, details of which can be found elsewhere.[14] The target used to produce CB_6^- and $C_2B_5^-$ was compressed from a 98% isotopically enriched ^{10}B powder mixed with ∼5% graphite. The PES resolution $\Delta E/E$ was ∼2.5%, i.e., ∼25 meV for 1 eV electrons. The spectra of CB_6^- and $C_2B_5^-$ at three different photon energies are presented in Figure 1. The spectra of both species are rather broad and complicated, indicating either large geometry changes in going from the anions to the neutrals and/or the presence of multiple isomers. The observed vertical detachment energies (VDEs) for the main PES bands are given in Table 1 and Tables S1 and S2 in the Supporting Information, where they are compared to theoretical data.

Computationally, we first searched for the global minima of CB_6^{2-}, CB_6^-, and $C_2B_5^-$ using the genetic algorithm program GEGA[15] at the B3LYP/3-21G level of theory. We then recalculated the geometries of low-lying isomers and two hexagonal structures of each species at the B3LYP/6-311+G* level of theory and those of the two lowest isomers of CB_6^- and $C_2B_5^-$ at the CCSD(T)/6-311+G* level. Total energies of the 12 local-minimum structures were recalculated at the CCSD(T)/6-311+G(2df)//B3LYP/6-311+G* level of theory.

[†] Utah State University.
[‡] Washington State University and Pacific Northwest National Laboratory.

10.1021/ja801211p CCC: $40.75

Table 1. Comparison of Experimental and Theoretical VDEs (eV) for CB_6^- and $C_2B_5^-$

structure	feature	exptl VDE[a]	final state; electronic configuration	theoretical VDE		
				TD-B3LYP	OVGF[b]	ΔCCSD(T)[c]
CB_6^- **V**	X tail	~2.9	$^1A'$; $(1a'')^2(7a')^2(8a')^2(2a'')^2(9a')^2(10a')^0$	3.20	3.19 (0.88)	2.95
	B	3.62(3)	$^3A'$; $(1a'')^2(7a')^2(8a')^2(2a'')^2(9a')^1(10a')^1$	3.65	3.56 (0.88)	3.68
	C	4.21(3)	$^3A''$; $(1a'')^2(7a')^2(8a')^2(2a'')^1(9a')^2(10a')^1$	4.14	4.11 (0.88)	4.22
	D	~4.5	$^1A''$; $(1a'')^2(7a')^2(8a')^2(2a'')^1(9a')^2(10a')^1$	4.55		
	E	4.71(5)	$^3A'$; $(1a'')^2(7a')^2(8a')^1(2a'')^2(9a')^2(10a')^1$	4.81	4.88 (0.86)	
CB_6^- **VI**	X[d]	2.78(3)	$^1A'$; $(1a'')^2(7a')^2(8a')^2(2a'')^2(9a')^2(10a')^0$	3.14	3.58 (0.88)	2.75
	A	3.17(2)	$^3A'$; $(1a'')^2(7a')^2(8a')^2(2a'')^2(9a')^1(10a')^1$	3.12	2.86 (0.88)	3.14
	C	4.21(3)	$^3A''$; $(1a'')^2(7a')^2(8a')^2(2a'')^1(9a')^2(10a')^1$	4.13	4.07 (0.88)	4.19
	D	~4.5	$^1A''$; $(1a'')^2(7a')^2(8a')^2(2a'')^1(9a')^2(10a')^1$	4.52		
	E	4.71(5)	$^3A'$; $(1a'')^2(7a')^2(8a')^1(2a'')^2(9a')^2(10a')^1$	4.74	4.78 (0.86)	
$C_2B_5^-$ **IX**	A	2.95(6)	$^2A_1$; $(1b_1)^2(4a_1)^2(5a_1)^2(1a_2)^2(4b_2)^2(6a_1)^1$	3.00	3.08 (0.88)	3.13
	C	4.36(4)	$^2B_2$; $(1b_1)^2(4a_1)^2(5a_1)^2(1a_2)^2(4b_2)^1(6a_1)^2$	4.42	4.73 (0.84)	4.49
	D	4.93(3)	$^2A_2$; $(1b_1)^2(4a_1)^2(5a_1)^2(1a_2)^1(4b_2)^2(6a_1)^2$	4.79	4.90 (0.88)	4.97
$C_2B_5^-$ **X**	X[d]	2.61(5)	$^2A'$; $(7a')^2(8a')^2(2a'')^2(9a')^2(10a')^1$	2.54	2.74 (0.86)	2.69
	B	4.06(3)	$^2A'$; $(7a')^2(8a')^2(2a'')^2(9a')^1(10a')^2$	4.13	4.47 (0.83)	

[a] Numbers in parentheses represent the uncertainty in the last digit. [b] VDEs were calculated at the OVGF/6-311+G(2df)//CCSD(T)/6-311+G* level of theory. Values in parentheses represent the pole strength of the OVGF calculation. [c] VDEs were calculated at the CCSD(T)/6-311+G(2df)//CCSD(T)/6-311+G* level of theory. [d] Experimental ADEs were estimated from the X band to be 2.71 ± 0.02 eV (CB_6^-) and 2.40 ± 0.05 eV ($C_2B_5^-$). Calculated ADE are 2.65 eV (CB_6^- **V**), 2.63 eV (CB_6^- **VI**), 2.82 eV ($C_2B_5^-$ **IX**), and 2.39 eV ($C_2B_5^-$ **X**) at the CCSD(T)/6-311+G(2df)//CCSD(T)/6-311+G* level.

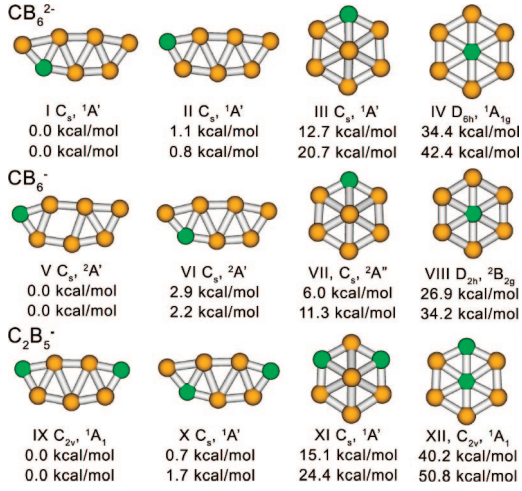

Figure 2. Calculated structures and relative energies for CB_6^{2-}, CB_6^-, and $C_2B_5^-$. The upper and lower values are from the CCSD(T)/6-311+G(2df)//B3LYP/6-311+G* and B3LYP/6−311+G* levels of theory, respectively.

VDEs for CB_6^- and $C_2B_5^-$ were calculated using the R(U)CCSD(T)/6-311+G(2df) method, the outer-valence Green's function method [ROVGF/6-311+G(2df)] at the RCCSD(T)/6-311+G* geometries, and the time-dependent DFT method [TD-B3LYP/6-311+G(2df)] at the B3LYP/6-311+G* geometries. All of the calculations were done using the Gaussian 03 program.[16a] Molecular orbital visualization was done using the MOLDEN3.4 program.[16b]

According to our GEGA search, the structure **I** (C_s) is the global minimum for CB_6^{2-} (Figure 2). Though the isolated CB_6^{2-} dianion is not electronically stable, as pointed out by Exner,[8a] we used the compact (6-311+G*) basis to model this unit in the electronically stable $NaCB_6^-$ or Na_2CB_6 species. This modeling was adequate for the description of the portion of the potential surface within the Coulomb barrier. The previously discussed[8a] structure **IV** (D_{6h}) with a hexacoordinate C is 34.4 kcal/mol higher in energy [here and elsewhere, the relative energies are given at the CCSD(T)/6-311+G(2df)//B3LYP/6-311+G* level] than the global minimum. Similarly, for CB_6^- and $C_2B_5^-$, the structures with a hexacoordinate C, **VIII** (D_{2h}) and **XII** (C_{2v}), are also significantly higher in energy than the corresponding global minima (Figure 2).

For all three clusters, we found a low-lying isomer very close to the global minimum. In the cases of CB_6^- and $C_2B_5^-$, the low-lying isomer may be present experimentally, giving rise to the complicated PES patterns. Indeed, comparison of the theoretical and experimental VDEs (Tables 1, S1, and S2) clearly shows that the two lowest isomers are almost equally populated for both CB_6^- and $C_2B_5^-$. For CB_6^-, the first VDEs for the two lowest isomers, **V** (2.95 eV) and **VI** (2.75 eV), calculated at the CCSD(T) level are close to each other, and both should contribute to the observed ground-state band X (Figure 1a−c). The first VDE of isomer **VI** is slightly lower, corresponding to the main X band, whereas that of isomer **V** corresponds to the higher-binding-energy tail of the X band. The second calculated VDEs for isomers **V** (3.68 eV) and **VI** (3.14 eV) are very different, corresponding to the observed PES bands B and A, respectively, and providing the most critical spectral signatures for the presence of the two isomers. Spectral features beyond 4 eV can all be assigned to the two isomers (Table S1).

For $C_2B_5^-$, the first four observed PES bands (Figure 1d−f) can be unambiguously assigned to the first two detachment channels of each of the two lowest isomers, as shown in Table 1. Higher PES bands can all be assigned to the higher-binding-energy detachment channels from the two isomers (the peak labeled * is likely due to a vibrational feature of the A band or a contribution from a third low-lying isomer), as given in Table S2. All of the observed PES bands are relatively broad without vibrational resolution, consistent with the low symmetries of the two isomers of each cluster and suggesting that these structures are relatively floppy. Overall, the agreement between the observed PES features and the theoretical data is quite satisfying and provides considerable credence for the lowest structures obtained for CB_6^- (**V** and **VI**) and $C_2B_5^-$ (**IX** and **X**). Clearly, the isomers with a hexacoordinate C (**VIII** for CB_6^- and **XII** for $C_2B_5^-$) are too high in energy. Though hypercoordinated isomers **IV** and **XII** are true local minima and kinetically stable, we were only able to observe the global minimum and low-lying isomers.

To understand why the structures with a hexacoordinate C for CB_6^{2-}, CB_6^-, and $C_2B_5^-$ are higher in energy than the corresponding global minima, we analyzed their chemical bonding using the recently developed adaptive natural density partitioning (AdNDP) method.[17] This approach leads to partitioning of the charge density into elements with the highest possible degree of localization of

electron pairs: *n*-center, two-electron (*n*c-2e) bonds. If some part of the density cannot be localized in this manner, it is represented using completely delocalized objects similar to canonical MOs, naturally incorporating the idea of completely delocalized (globally aromatic) bonding. Thus, AdNDP achieves a seamless description of different types of chemical bonds.

According to our AdNDP analyses (see Figures S4 and S5 in the Supporting Information for details), the hexagonal structures of CB_6^{2-} and $C_2B_5^-$ are doubly (σ- and π-) aromatic systems (six delocalized σ electrons and six delocalized π electrons) with six peripheral 2c-2e B−B or B−C bonds. This bonding picture explains why the hexagonal isomers with a central C atom (**IV** and **XII**) are higher in energy than those with the C atoms located on the periphery (**III** and **XI**). The central C atoms in **IV** and **XII** are involved in delocalized bonding only, while the C atoms in **III** and **XI** are involved in 2c-2e peripheral bonding in addition to the delocalized bonding. The lower electronegativity of B compared to C clearly favors the hexacoordinate B isomers of CB_6^{2-} and $C_2B_5^-$.

The lowest-energy structures for CB_6^{2-} (**I** and **II**) and $C_2B_5^-$ (**IX** and **X**) originate from heptacyclic structures. These four structures are all σ-aromatic (six delocalized σ electrons) and π-antiaromatic (four π electrons) and have seven peripheral 2c-2e B−B/B−C bonds. There are no "internal" 2c-2e B−B or B−C bonds; in Figure 2, the internal lines connecting atoms do not represent 2c-2e B−B or B−C bonds. In order to prove that these low-symmetry structures are indeed related to seven-membered rings, we performed additional calculations for the CB_6 cluster. We started by removing two electrons from the HOMO (10a′) of the CB_6^{2-} global-minimum structure **I** (Figure S6 in the Supporting Information). In the resulting neutral CB_6 structure, we switched the σ-HOMO (9a′) and π-LUMO+2 (3a″), making this structure doubly aromatic (two σ electrons and six π electrons) and preserving seven 2c-2e peripheral B−B/B−C bonds. Subsequent geometry optimization of the doubly aromatic structure led to an almost perfect heptagonal ring for CB_6 (C_{2v}, $^1A_1$) (Figure S6). The MOs of the latter now clearly confirm our initial assignment of this cluster as doubly aromatic (two σ electrons and six π electrons) with seven 2c-2e peripheral B−B/B−C bonds. Hence, the stable, low-lying structures **I** and **II** for CB_6^{2-} and **IX** and **X** for $C_2B_5^-$ are derived from distortions of the heptacyclic structures due to π antiaromaticity. There may be more than one deformation of the C_{2v} CB_6 after addition of two electrons. We selected the above-mentioned one for illustrative purposes.

Our chemical bonding analyses suggest that in the theoretical design of chemical systems with planar hypercoordination, the peripheral ring size and the electronegativity and size of the central atom must all be considered.[6a] The highest coordination number observed to date in a planar environment is 8, in the B_9^- molecular wheel.[18] A similar molecular wheel with a nonacoordinate Al has been predicted for AlB_9,[19] currently representing the highest coordination number in the planar environment achievable in a low-energy isomer.

Acknowledgment. The experimental work done at Washington State University was supported by the National Science Foundation (DMR-0503383) and performed at the W. R. Wiley Environmental Molecular Sciences Laboratory, a national scientific user facility sponsored by DOE's Office of Biological and Environmental Research and located at Pacific Northwest National Laboratory, which is operated for DOE by Battelle. The theoretical work done at Utah State University was supported by the National Science Foundation (CHE-07148510).

Supporting Information Available: Complete ref 16a; alternative structures of CB_6^{2-}, CB_6^-, and $C_2B_5^-$; pictures of *n*c-2e localized bonds for CB_6^{2-} and $C_2B_5^-$ structures; an MO correlation diagram; complete VDE tables; and absolute energies and Cartesian coordinates for all of the calculated structures. This material is available free of charge via the Internet at http://pubs.acs.org.

References

(1) (a) Hoffmann, R.; Alder, R. W.; Wilcox, C. F., Jr *J. Am. Chem. Soc.* **1970**, *92*, 4992. (b) Hoffmann, R. *Pure Appl. Chem.* **1971**, *28*, 181.
(2) Keese, R. *Chem. Rev.* **2006**, *106*, 4787, and references therein.
(3) Merino, G.; Mendez-Rojas, M. A.; Vela, A.; Heine, T. *J. Comput. Chem.* **2007**, *28*, 362, and references therein.
(4) Sateesh, B.; Reddy, A. S.; Sastry, G. N. *J. Comput. Chem.* **2007**, *28*, 335, and references therein.
(5) Siebert, W.; Gunale, A. *Chem. Soc. Rev.* **1999**, *28*, 367, and references therein.
(6) (a) Schleyer, P. v. R.; Boldyrev, A. I. *J. Chem. Soc. Chem. Comm.* **1991**, 1536. (b) Boldyrev, A. I.; Simons, J. *J. Am. Chem. Soc.* **1998**, *120*, 7967.
(7) (a) Li, X.; Wang, L. S.; Boldyrev, A. I.; Simons, J. *J. Am. Chem. Soc.* **1999**, *121*, 6033. (b) Wang, L. S.; Boldyrev, A. I.; Li, X.; Simons, J. *J. Am. Chem. Soc.* **2000**, *122*, 7681. (c) Li, X.; Zhang, H. F.; Wang, L. S.; Geske, G. D.; Boldyrev, A. I. *Angew. Chem., Int. Ed.* **2000**, *39*, 3630. (d) Li, X.; Zhai, H. J.; Wang, L. S. *Chem. Phys. Lett.* **2002**, *357*, 415.
(8) (a) Exner, K.; Schleyer, P. v. R. *Science* **2000**, *290*, 1937. (b) Wang, Z.-X.; Schleyer, P. v. R. *Science* **2001**, *292*, 2465. (c) Erhardt, S.; Frenking, G.; Chen, Z.; Schleyer, P. v. R. *Angew. Chem., Int. Ed.* **2005**, *44*, 1078. (d) Ito, K.; Chen, Z.; Corminboeuf, C.; Wannere, C. S.; Zhang, X. H.; Li, Q. S.; Schleyer, P. v. R. *J. Am. Chem. Soc.* **2007**, *129*, 1510. (e) Islas, R.; Heine, T.; Ito, K.; Schleyer, P. v. R.; Merino, G. *J. Am. Chem. Soc.* **2007**, *129*, 14767.
(9) (a) Minyaev, R. M.; Gribanova, T. N.; Starikov, A. G.; Minkin, V. I. *Mendeleev Commun.* **2001**, *11*, 213. (b) Gribanova, T. N.; Minyaev, R. M.; Minkin, V. I. *Russ. J. Inorg. Chem.* **2001**, *46*, 1207. (c) Minyaev, R. M.; Gribanova, T. N.; Starikov, A. G.; Minkin, V. I. *Dokl. Chem.* **2002**, *382*, 41. (d) Minkin, V. I.; Minyaev, R. M. *Mendeleev Commun.* **2004**, *14*, 43.
(10) (a) Li, S.-D.; Miao, C.-Q.; Ren, G.-M. *Eur. J. Inorg. Chem.* **2004**, 2232. (b) Li, S.-D.; Guo, J.-G.; Miao, C.-Q.; Ren, G.-M. *J. Phys. Chem. A* **2005**, *109*, 4133. (c) Li, S.-D.; Miao, C.-Q. *J. Phys. Chem. A* **2005**, *109*, 7594. (d) Li, S.-D.; Miao, C.-Q.; Ren, G.-M.; Guo, J.-C. *Eur. J. Inorg. Chem.* **2006**, 2567. (e) Shahbazian, S.; Sadjadi, A. *THEOCHEM* **2007**, *822*, 116.
(11) Kemsley, J. *Chem. Eng. News* **2007**, *85* (33), 17.
(12) (a) Luo, Q.; Zhang, X. H.; Huang, L. K.; Liu, S. Q.; Yu, Z. H.; Li, Q. S. *J. Phys. Chem. A* **2007**, *111*, 2930. (b) Li, S.-D.; Miao, C.-Q.; Guo, J.- C. *J. Phys. Chem. A* **2007**, *111*, 12069.
(13) Wang, L. M.; Huang, W.; Averkiev, B. B.; Boldyrev, A. I.; Wang, L. S. *Angew. Chem., Int. Ed.* **2007**, *46*, 4550.
(14) Wang, L. S.; Cheng, H. S.; Fan, J. *J. Chem. Phys.* **1995**, *102*, 9480.
(15) (a) Alexandrova, A. N.; Boldyrev, A. I.; Fu, Y.-J.; Wang, X. B.; Wang, L. S. *J. Chem. Phys.* **2004**, *121*, 5709. (b) Alexandrova, A. N.; Boldyrev, A. I. *J. Chem. Theory Comput.* **2005**, *1*, 566.
(16) (a) Frisch, M. J. Gaussian 03, revision D.01; Gaussian, Inc.: Wallingford, CT, 2004. (b) Schaftenaar, G. MOLDEN3.4; CAOS/CAMM Center: Nijmegen, The Netherlands, 1998.
(17) Zubarev, D. Y.; Boldyrev, A. I. *Phys. Chem. Chem. Phys.*, accepted for publication.
(18) (a) Zhai, H. J.; Alexandrova, A. N.; Birch, K. A.; Boldyrev, A. I.; Wang, L. S. *Angew. Chem., Int. Ed.* **2003**, *42*, 6004. (b) Alexandrova, A. N.; Boldyrev, A. I.; Zhai, H.-J.; Wang, L. S. *Coord. Chem. Rev.* **2006**, *250*, 2811. (c) Zubarev, D. Y.; Boldyrev, A. I. *J. Comput. Chem.* **2007**, *28*, 251.
(19) Averkiev, B. B.; Boldyrev, A. I. *Russ. J. Gen. Chem.* **2008**, *78*, 769.

JA801211P